Available online at www.sciencedirect.com
ScienceDirect
Trans. Nonferrous Met. Soc. China 22(2012) 1517−1525
Transactions of Nonferrous Metals Society of China
www.tnmsc.cn

Numerical simulation of flow characteristics in settler of flash furnace

ZHOU Jun[1], CHEN Zhuo[2, 3], ZHOU Ping[2, 3], YU Jian-ping[2], LIU An-ming[4]

1. School of Metallurgical Science and Engineering, Central South University, Changsha 410083, China;
2. School of Energy Science and Engineering, Central South University, Changsha 410083, China;
3. Hunan Key Laboratory of Energy Conservation in Process, Changsha 410083, China;
4. Jinlong Copper Co. Ltd., Tongling 244021, China

Received 10 February 2012; accepted 16 May 2012

Abstract: A computational fluid dynamics (CFD) simulation was carried out with CFX4.3 to investigate the melt flow and temperature distributions in the settler of a flash furnace. Sixteen cases of one slag tap hole adopted with one matte tap hole (1-to-1) and one slag tap hole adopted with two matte tap holes (1-to-2) operation modes were modelled. The simulation results show that the melt flows are similar in both two operation modes, but evident circulations can be found in the case of the 1-to-2 operation mode. The combination modes of the slag and matte tap holes are found to have a significant effect on the temperature distributions of the melt. The melt temperature is more uniform in the case of the 1-to-2 mode. Selection of a matte tap hole farther away from the inlet is more conducive to achieve a uniform distribution of the melt temperature in the settler in practical tapping operation.
Key words: CFD simulation; melt flow; melt temperature; settler; flash smelting

1 Introduction

In the past decades, the Outokumpu copper flash smelting process has witnessed great progresses in the high concentrate throughputs, good control of copper loss and improved furnace designs. In particular, as a result of the application of oxygen enrichment and high matte grade production, the productivities of most flash smelting furnaces have been doubled or even tripled in comparison with their original designed capacities [1]. Until the end of last century, approximately half of the world primary copper has been produced through the Outokumpu flash smelting technology.

The high throughput of the furnace however also brings about many problems for the furnace operation. For instance, the copper losses through the slag were found to increase, un-smelted materials piled up more frequently under the reaction shaft, the brick-lining eroded faster, and the accretion in the settler became thick so that the effective volume was not enough for a good separation of the melt and the slag. Some of the problems are obviously the results of incomplete reactions in the reaction shaft, while some are related to the melt flow and separations inside the settler.

Research on the flash furnace has been most concentrated on study of the smelting process, such as numerical simulations by JORGENSEN and KOH [2], LI et al [3] and SOLNORDAL et al [4] using different computational fluid dynamics (CFD) softwares, and the development of the artificial intelligent model by GUI et al [5] for predictions of matte grades of the flash smelting production. Meanwhile, great efforts have also been put on improvement of the concentrate burner. CHEN and MEI [6] proposed some optimizations of the burner operation by CFD simulation; XIE [7] made a detailed study on the design and performance of a swirling burner; KON et al [8], DEBRINCAT et al [9, 10] and HIGGINS et al [11] investigated the particle agglomeration in the reaction shaft from either numerical modelling or experiments. Comparing with lots of work reported on the smelting reactions and equipment improvements, the literature survey revealed very little information concerning the matte- and slag-forming processes in the settler of the furnace. Experimental studies [12, 13] and numerical modeling [14] had been ever carried out on the separation and phase formation of the smelting mixtures, but few references could be found

Foundation item: Project (2002AA00104) supported by the National High-tech Research and Development Program of China
Corresponding author: CHEN Zhuo; Tel/Fax: +86-731-88879863; E-mail: chenzhuo@csu.edu.cn
DOI: 10.1016/S1003-6326(11)61350-2

about the study of the flow characteristic and temperature distribution of the melt in the settler. Thus, a numerical simulation was carried out with CFX4.3, aiming to optimize the tapping operation scheme and to improve the separation of the matte and the slag on the basis of the research results.

2 Numerical model

2.1 Computational geometry

The computational geometry of the study includes only the melt part of the settler of a flash smelting furnace, of which the annual throughput is 2.5×10^5 t anode copper. The computational domain is 22.6 m in length, 6.3 m in width and 1.05 m in depth. The industrial test and previous numerical simulations have revealed that most melted particles entered the settler from a round area of 3 m in diameter though the diameter of the reaction shaft outlet was 5.5 m [7, 15]. Hence, a round surface of 3 m in diameter was made on the top of the computational domain as the inlet for the melt droplets falling from the reaction shaft into the settler.

There are four matte tap holes along the south side of the settler and two slag tap holes at the far end below the uptake shaft (U/T side, as shown in Fig. 1). To distinguish these six tap holes in following study, the four matte tap holes are labelled as M1 to M4, according to their positions away from the reaction shaft side (R/S side, as illustrated in Fig. 1), and the two slag tap holes are referred to SS and SN, respectively, which mean the "slag hole at south side" and the "slag hole at north side". Although these tap holes are run alternatively in practice, they are assumed to be in a continuous operation and steady-state in the computation since there are only very short intervals between the switching operations.

The multi-block structured meshes are adopted for the computational domain, as displayed in Fig. 2. Local finer grids are used in the settler's inlet and the four matte taping holes in order for a careful investigation of the melt flow in these areas.

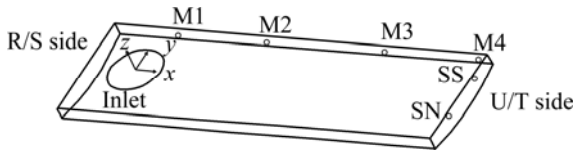

Fig. 1 Computational geometry of settler

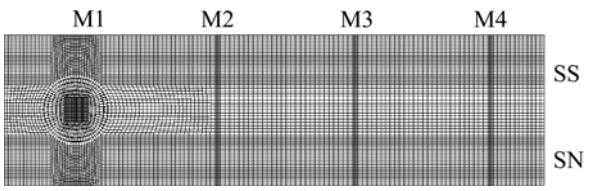

Fig. 2 Meshes used for computation (M1, M2, M3, M4—Matte exits; SN, SS—Slag exits)

2.2 Mathematical model

In the Outokump flash smelting process, the concentrate particles react and melt into droplets when they are falling through the reaction shaft. Upon the melt surface in the settler, the droplets merge into the liquid phase (the melt) quickly. When flowing towards the tap holes, the matte goes down to the bottom whilst the slag keeps floating on the surface, forming two layers of the melt in the settler due to their density differences. As the slag layer is much thinner than the matte layer, the slag is included in the matte layer in the computation, and the melt is then simplified to be only the matte by ignoring the density difference between the two phases.

Based on the above simplifications, a steady-state, incompressible, turbulent flow numerical model is developed to investigate the melt motion in the flash smelting furnace (FSF) settler with CFX 4.3. The governing equations include the continuity, momentum and heat transfer equations.

Continuum equation:

$$\frac{\partial}{\partial x_i}(\rho u_i)=0 \tag{1}$$

Momentum equation:

$$\frac{\partial}{\partial x_j}(\rho u_j u_i)=-\frac{\partial p}{\partial x_i}+\frac{\partial}{\partial x_j}\left[\mu_{\mathrm{e}}\left(\frac{\partial u_i}{\partial x_j}+\frac{\partial u_j}{\partial x_i}\right)\right]+\rho g_i \tag{2}$$

Energy equation:

$$\frac{\partial}{\partial x_i}(\rho u_i H)=\frac{\partial}{\partial x_i}\left[\left(\frac{\lambda}{c_p}+\frac{\mu_{\mathrm{e}}}{\sigma_H}\right)\cdot\frac{\partial H}{\partial x_i}\right] \tag{3}$$

κ—ε equations:

$$\frac{\partial}{\partial x_i}(\rho k u_i)=\frac{\partial}{\partial x_j}\left[\left(\mu+\frac{\mu_t}{\sigma_k}\right)\cdot\frac{\partial k}{\partial x_j}\right]+G_k+G_{\mathrm{b}}-\rho\varepsilon \tag{4}$$

$$\frac{\partial}{\partial x_i}(\rho\varepsilon u_i)=\frac{\partial}{\partial x_j}\left[\left(\mu+\frac{\mu_t}{\sigma_\varepsilon}\right)\cdot\frac{\partial \varepsilon}{\partial x_j}\right]+C_{1\varepsilon}\frac{\varepsilon}{k}G_k-C_{2\varepsilon}\rho\frac{\varepsilon^2}{k} \tag{5}$$

where ρ is the melt density; u_i and u_j are the velocity components; p is the static pressure; H is the enthalpy; λ is the melt conductivity; c_p is the specific heat capacity of the melt; κ is the turbulent kinetic energy; G_k is the component of the turbulent kinetic energy caused by velocity gradient; G_{b} is the component of the turbulent kinetic energy caused by buoyancy; ε is the turbulent kinetic energy dissipation rate; σ_H, σ_k and σ_ε are the Prantdl number of turbulence respectively in the enthalpy equation and the κ—ε equations [16]; μ_{e}, the effective viscosity, is the sum of the molecular viscosity μ and the turbulent viscosity μ_{t}, namely, $\mu_{\mathrm{e}}=\mu+\mu_{\mathrm{t}}$, in which

$$\mu_{\mathrm{t}}=\rho C_\mu\frac{k^2}{\varepsilon} \tag{6}$$

where C_μ, $C_{1\varepsilon}$, $C_{2\varepsilon}$, σ_k and σ_ε in above equations are constant, and their usual values are

C_μ=0.09, $C_{1\varepsilon}$=1.44, $C_{2\varepsilon}$=1.92, σ_k=1.0 and σ_ε=1.3.

2.3 Boundary conditions

The boundary conditions include the numerical settings for the inlet, the outlet, the melt surface and the surrounding walls of the computational domain.

The mass flow rate of the melt at the inlet is 24.2 kg/s and its average falling speed is 2.8 m/s. The melt coming down from the reaction shaft is at a high temperature of about 1700 K. As the melt enters the settler in a disperse state which cannot be correctly described by the module provided in the software, an UDF code was developed to define the details of the mass flux and the velocity distribution of the melt droplets around the inlet of the settler [17].

The outlet is set to be the pressure outlet and a gauge pressure of 0 Pa is specified. As the melt surface is the interface of the flue gas and the melt in the settler, the surface is treated as a free surface in the numerical model. All walls including the side walls and the bottom of the computational domain are set to be no-slip walls, of which the k and ε are calculated with the wall function. The temperatures of all walls are set to be the melting point of the matte.

3 Discussions and analysis of computational results

In general, the two slag tap holes are run alternatively with one or two matte tap holes. Therefore, there are eight cases for the operations when one slag tap hole is run with one matte tap hole (referred to as the 1-to-1 mode). For the operations of one slag tap hole run simultaneously with two matte tap holes (referred to as the 1-to-2 mode), though there should be twelve cases for all the combinations, only eight are used in general operations and the other four are seldom adopted. These usual eight cases are also included in the computation. Hence, there are altogether sixteen cases that have been modelled in the study to investigate the characteristics of the melt motion and temperature distributions at different combinations of the matte and slag tap holes.

3.1 Results of 1-to-1 mode

3.1.1 Results of melt flow in 1-to-1 mode

A typical results of the melt flow in the 1-to-1 operation mode are given in Fig. 3, in which the SN slag tap hole is run together with M1 matte tap hole (referred to as the M1-SN in the text).

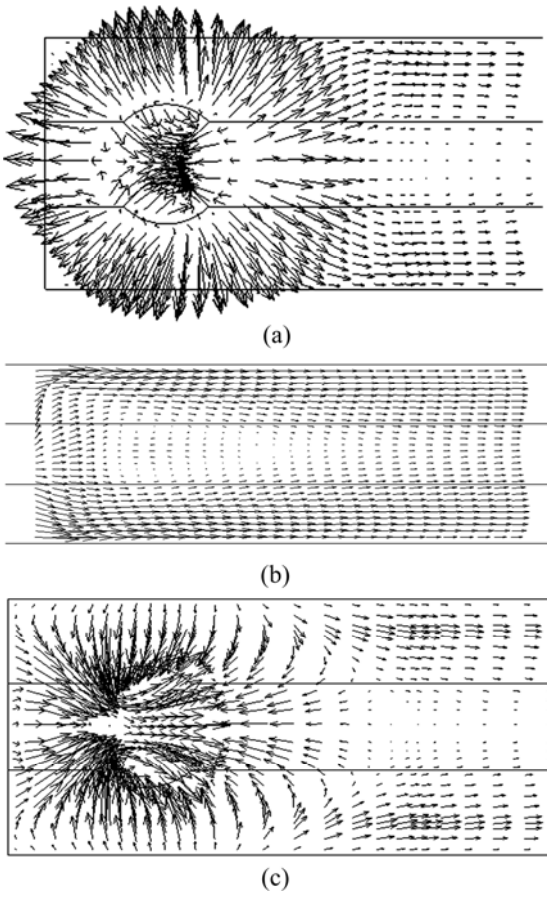

Fig. 3 Velocity vectors of melt flow in cross-section of different depths in settler: (a) Velocity vectors in cross-section of z=−0.2 m; (b) Enlarged velocity vectors in cross-section of z=−0.5 m; (c) Velocity vectors in cross-section of z=−0.7 m

As illustrated in Fig. 3, the melted droplets fall into the settler at a high velocity of about 2.8 m/s. Impinged by the fast droplets, the melt in the settler exhibits a chaotic flow in the inlet region. On the surface of the settler, the melt is pushed away by the high speed gas and droplet flow, first moving radially, then turning back to go along the melt bulk since it is obstructed by the walls. The melt deep inside the settler is strongly stirred under the impact of the gas and droplets, with the stuff at the bottom being carried upwards to the surface along the side walls, then moving to the downstream of the settler.

In is shown in Fig. 4 the velocity contours of multiple sections along the settler's length. It can be clearly seen that the melt near the side walls flows faster than that in the centre of the settler. In particular, the local melt velocity in the central region near to the inlet is extremely low, or even approaches to be of no motion. This uneven distribution of the melt velocity implies a possibility that the melt (especially the slag) takes a short-cut to the exit of the settler, which is the SN slag tap hole in this case.

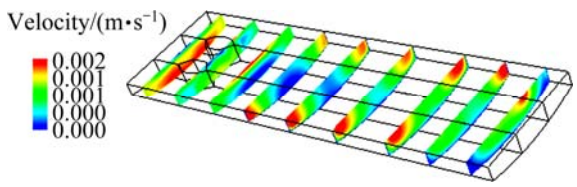

Fig. 4 Velocity contours of cross-sections along settler

Results of the flow fields of all the eight cases of the 1-to-1 operation mode are displayed in Fig. 5, which indicates that different combinations of the matte and slag tap holes have a great influence on the melt flow in the settler. To make a quantitative analysis of the melt flow in different cases, the term "dead zone" is borrowed to define the regions where the melt velocity is extremely low. As the average melt velocity in usual design of the settler is 2.5 mm/s, the velocity limit of the "dead zone" is set to be 0.5 mm/s in the study. With such a velocity, the average residence time of the melt staying in the settler will be over 11 h, which is much more than the time needed for a complete separation of the matte and the slag. By adding all the volume of the grids in which the melt velocity is lower than 0.5 mm/s, the volume of the dead zone as well as the fraction of the dead zone to the settler's total volume can be obtained in all cases.

As listed in Table 1, the dead zones in the case of one matte tap hole combined with the northern slag exit are generally larger than those in the case when the slag is tapped from the southern exit. The primary reason is that the flow path is apparently longer when the melt exits from the northern slag tap hole since all the matte tap holes are on the south of the settler. A short-cut of the melt flow is more easily formed in the centre and the northern side of the settler, whilst the melt in the downstream of the south keeps a motion of low speed due to few disturbances resulted from the bulk flow. Moreover, in all four cases when the matte tap holes are combined with the same slag tap hole, the dead zone fraction decreases when the matte tap hole stays farther away to the inlet (or in other word, becomes even closer

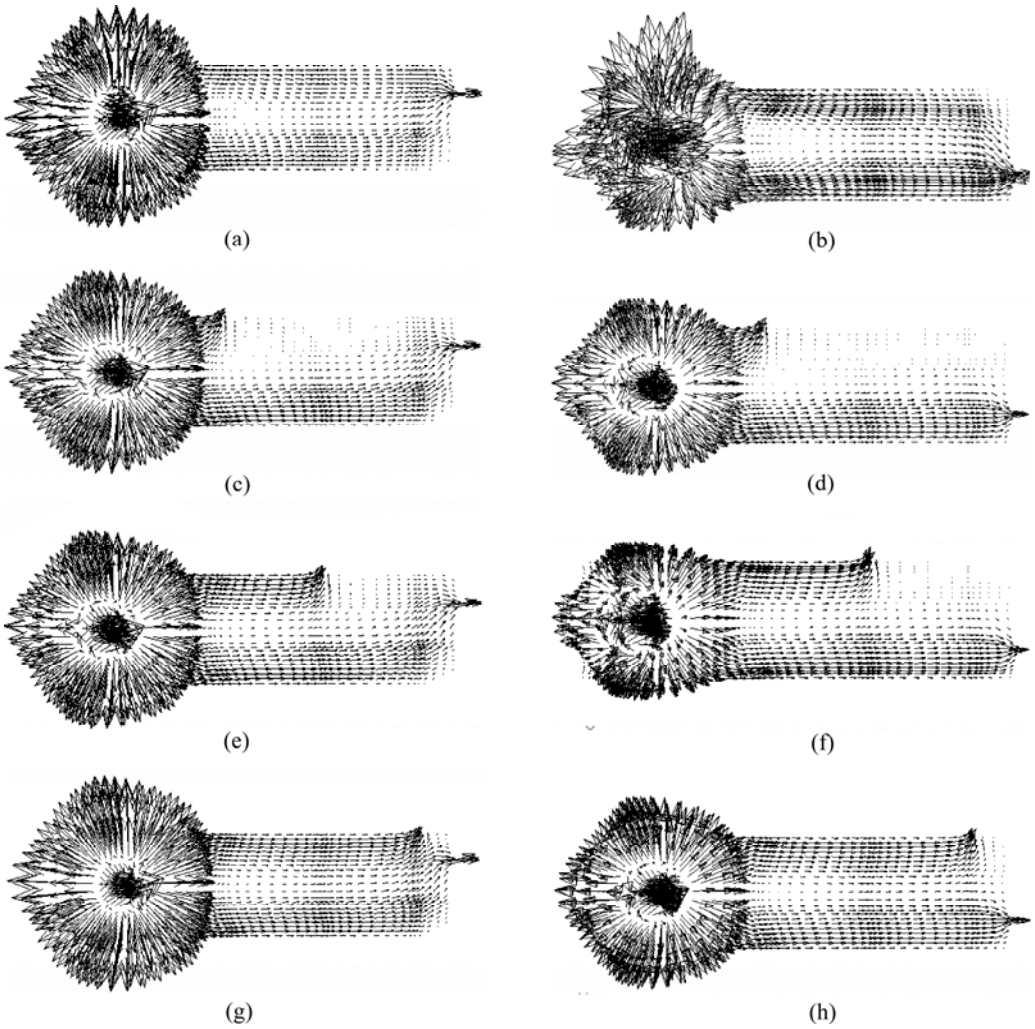

Fig. 5 Velocity vectors of eight cases in 1-to-1 operation mode: (a) M1-SN; (b) M1-SS; (c) M2-SN; (d) M2-SS; (e) M3-SN; (f) M3-SS; (g) M4-SN; (h) M4-SS

Table 1 Volume fraction of dead zone in the case of 1-to-1 operation mode

One matte taping holes run with SN/SS slag tap hole	Volume fraction of dead zone/%
M1-SN	38.82
M2-SN	38.75
M3-SN	30.60
M4-SN	17.07
M1-SS	34.94
M2-SS	34.88
M3-SS	27.54
M4-SS	15.36

to the slag exit). As the result, the maximum of the dead zone in the 1-to-1 operation mode occurs in the case of M1-SN, while the minimum happens in the case of M4-SS, as given in Table 1.

3.1.2 Results of melt temperature in 1-to-1 mode

Simulation results indicate that the melt flow has a significant influence on the distribution of the melt temperature in the settler. As shown in Fig. 6, the melt temperature near the inlet is higher that in the centre and it exhibits a great temperature gradient, due to the impact of the high speed gas and melt-droplets falling into the settler. When moving downwards, the temperature gradient along the settler's cross-sections decreases, with a low temperature in the centre and along the side walls, whilst it is relatively high in the in-between of the low temperature regions. Consulting the results of the melt flow in the same melt layer (as given in Fig. 3(b)), it can be found that the high temperature region corresponds to the strong melt motion region, while the low temperature region is mainly the area of low melt velocity, especially in the downstream of the setter.

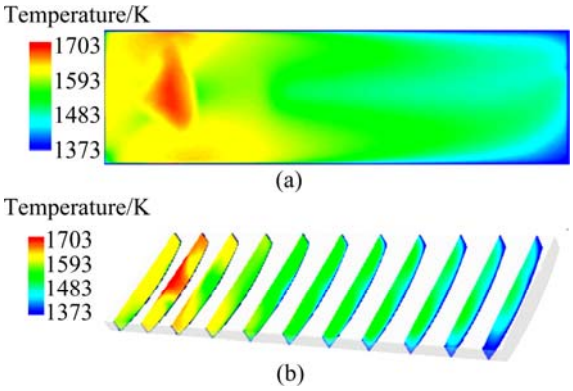

Fig. 6 Temperature contours in multi-sections in settler: (a) Temperature contour in cross-section of z=−0.5 m; (b) Temperature contours of cross-section along settler

Further analysis is made by comparison of the eight temperature results in 1-to-1 mode, as shown in Fig. 7. Considering that the normal matte tapping temperature is 1473 K, a "low temperature zone" is defined as the region where the melt temperature is lower than 1473 K. With such a definition, fractions of the low temperature zones of all eight cases are summarized in Table 2. In the four cases when the southern slag exit is adopted, the low temperature zones are generally smaller than those of the cases where the northern slag tap hole is in use, due to the flow characteristics in the cases explained above. It is

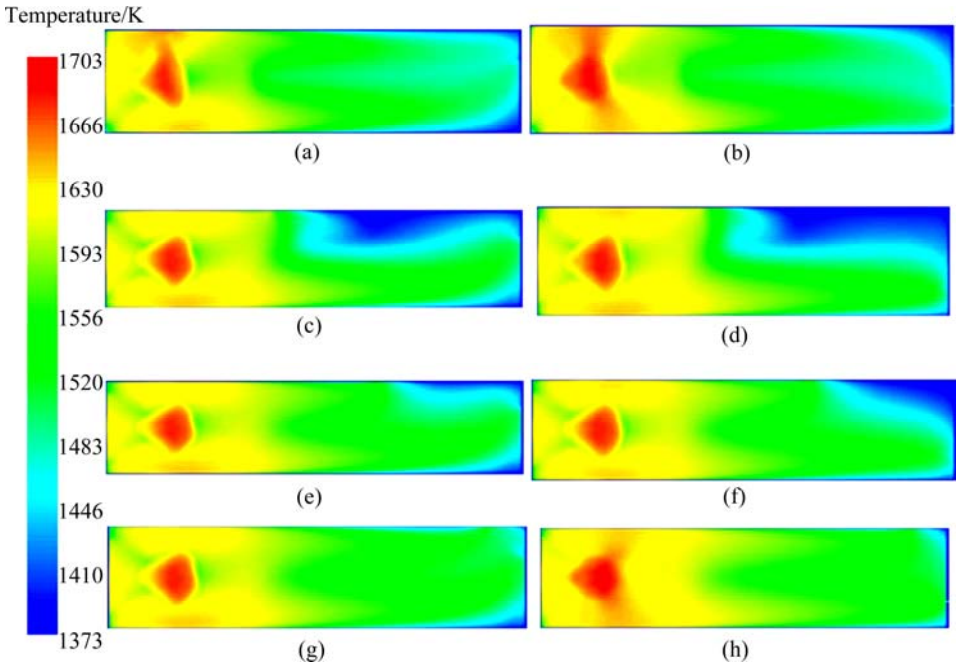

Fig. 7 Temperature contours in 1-to-1 operation mode: (a) M1-SN; (b) M1-SS; (c) M2-SN; (d) M2-SS; (e) M3-SN; (f) M3-SS; (g) M4-SN; (h) M4-SS

Table 2 Volume fractions of low temperature zones in 1-to-1 operation mode

One matte taping holes run with SN/SS slag tap hole	Volume fraction of low temperature zone/%
M1-SN	19.25
M2-SN	25.40
M3-SN	12.84
M4-SN	8.23
M1-SS	17.33
M2-SS	22.86
M3-SS	11.55
M4-SS	7.41

also found that the fractions are usually small when the M4 tap hole is used with either slag exits, and they become large when the M2 is adopted.

The simulation results of matte temperature at different tap holes are listed in Table 3. Compared with the measured matte tapping temperature of 1508−1515 K, the error of the simulated melt temperature is estimated to be about 2%. Moreover, it can be found that the matte temperature varies with the matte tap hole, and the nearer the hole lies to the inlet, the higher the matte temperature is. Therefore, the selection of a proper hole for the matte tapping operation seems to be a possible effective measure for a mild adjustment of the matte temperature in the settler. Concluded with analysis of both the flow and temperature results, it is suggested to choose M3 or M4 (i.e., the matte tap holes far away to the inlet) for the practical matte tapping operation.

Table 3 Matte temperatures at different tap holes (in the case of M1-SS)

Matte tap hole	M1	M2	M3	M4
Matte temperature/K	1537	1520	1504	1483

3.2 Results of 1-to-2 mode

3.2.1 Results of melt velocity in 1-to-2 mode

As shown in Fig. 8, the melt flow in the 1-to-2 mode is also chaotic at the inlet of the settler. But with two matte tap holes put in use, evident circulations can be found near the inlet region, moving from the settler's sides to the centre. In the downstream of the settler, the melt velocity is obviously low in the centre and relatively high along the two side walls. As a result, the melt seems more likely to take a shortcut through either the matte tap holes or the slag exit, especially for cases when the matte tap holes are adopted together with the northern slag exit.

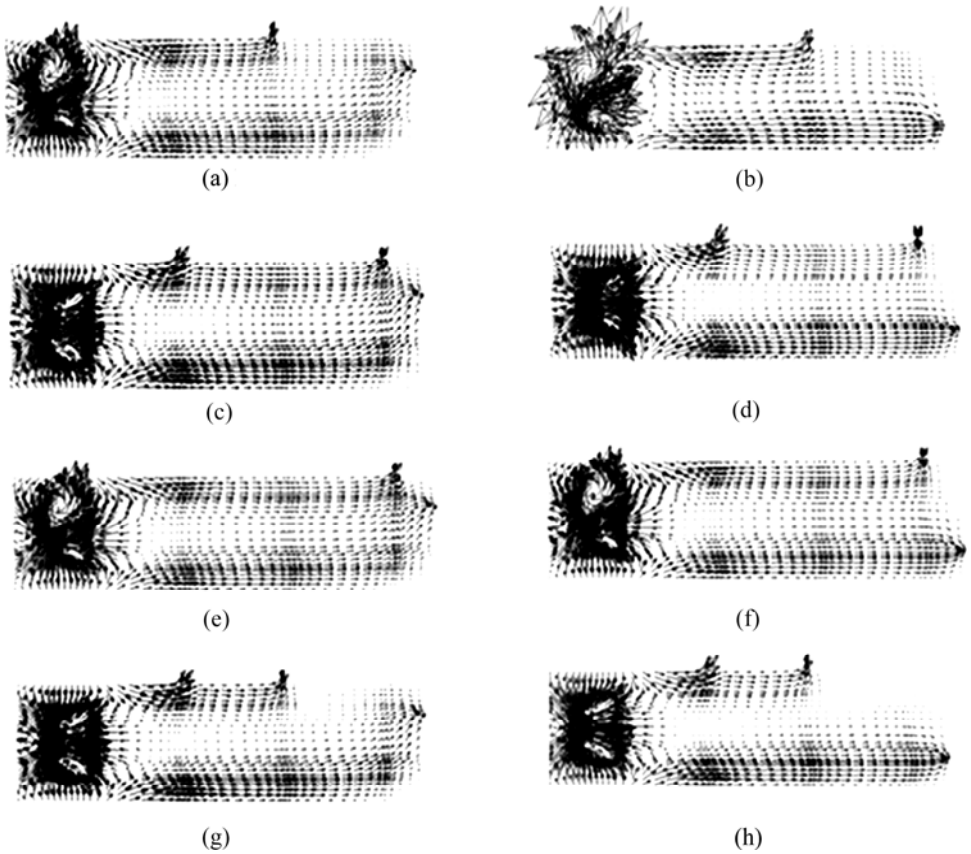

Fig. 8 Velocity vectors of cases in 1-to-2 mode: (a) M1-M3-SN; (b) M1-M3-SS; (c) M2-M4-SN; (d) M2-M4-SS; (e) M1-M4-SN; (f) M1-M4-SS; (g) M2-M3-SN; (h) M2-M3-SS

Furthermore, for all eight cases computed in the study, the flow fields of M2-M4-SS, M1-M4-SS, M2-M4-SN and M1-M4-SN are comparatively more uniform, with a central slow flow surrounded with high melt velocity along the walls. However, when the M3 matte tap hole is in use, large low-velocity areas are found in the downstream, near the southern side wall and the settler's end. The dead zones calculated for these cases are clearly larger than the other four cases, as given in Table 4.

Table 4 Volume fractions of dead zones in 1-to-2 operation mode

Two matte taping holes run with SN/SS slag tap hole	Volume fraction of dead zone/%
M1-M3-SN	35.95
M2-M4-SN	26.61
M1-M4-SN	31.24
M2-M3-SN	37.31
M1-M3-SS	34.14
M2-M4-SS	26.91
M1-M4-SS	23.58
M2-M3-SS	34.35

It is worth noticing that, compared with the values in the 1-to-1 mode, the fractions of the dead zones become smaller when M1 or M2 is used with either of the other two matte tap holes downstream, whilst it is larger when M3 or M4 is used in combination of one of the matte tap holes upstream. The differences indicate that combinations of the matte and slag tap holes have significant effects on the melt flow in the settler. It is then feasible to optimize the residence time of the melt and the separation between the matte and slag by choosing proper exits for the tapping operation.

3.2.2 Results of melt temperature in 1-to-2 mode

Simulation results of the melt temperature in the 1-to-2 mode are given in Fig. 9. Similar to cases when single matte tap hole is adopted, the highest temperature in these cases still appears at the inlet region, but it soon becomes uniform across the cross-section when the melt moves downwards along the settler. As a result, large temperature gradient occurs mainly in a small area near the inlet, while long uniform temperature distribution is formed in the remaining part of the settler. It is also found that the variation in the low temperature zones exhibits similar trend to that in the melt flow. As listed in Table 5, the fractions of the low temperature zones are larger when the upstream tap hole M1 or M2 is used together with any one of the downstream matte exits (M3 or M4), compared with cases when only M1 or M2 tap hole is used solely. However, the figures become smaller when M3 (or M4) is adopted in combination with M1 or M2 in upstream, compared with corresponding cases when M3 or M4 is used alone. The maximum of the low temperature zone in the 1-to-2 mode is found in the case of M2-M3-SN, and the minimum fraction occurs in the case of M2-M4-SS. But the difference between these two figures is less significant than that in the mode of 1-to-1,

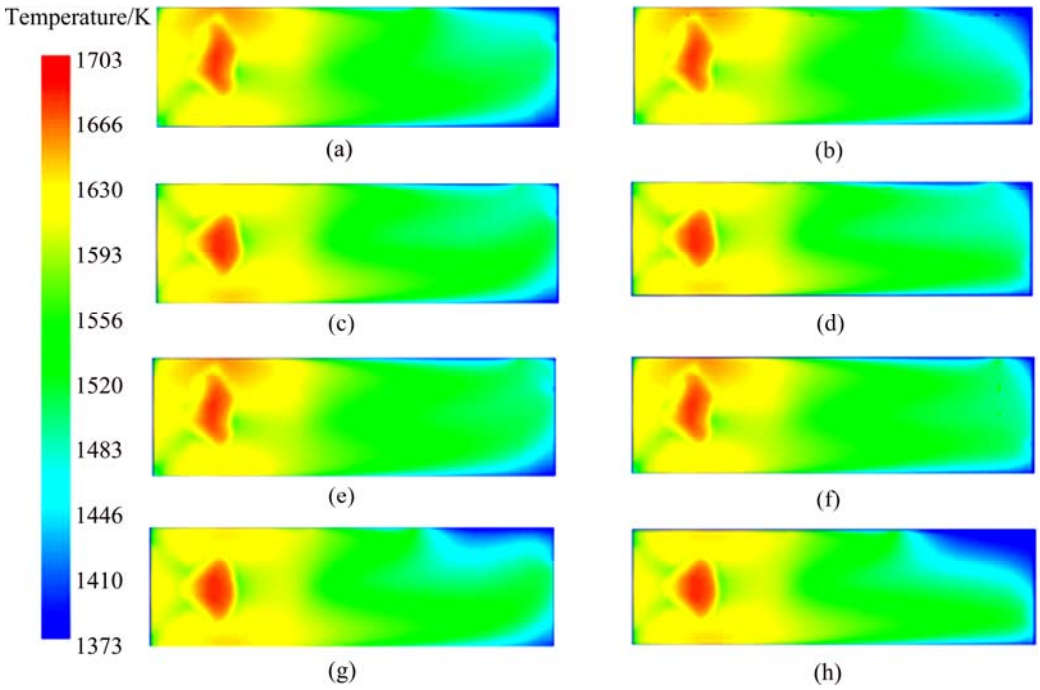

Fig. 9 Temperature contours in settler cross-section in 1-to-2 mode: (a) M1-M3-SN; (b) M1-M3-SS; (c) M2-M4-SN; (d) M2-M4-SS; (e) M1-M4-SN; (f) M1-M4-SS; (g) M2-M3-SN; (h) M2-M3-SS

Table 5 Volume fraction of low temperature zones in 1-to-2 operation mode

Two matte taping holes run with SN/SS slag tap hole	Volume fraction of low temperature zone/%
M1-M3-SN	15.90
M2-M4-SN	11.28
M1-M4-SN	11.76
M2-M3-SN	18.65
M1-M3-SS	14.17
M2-M4-SS	10.75
M1-M4-SS	11.79
M2-M3-SS	15.30

which shows that the melt temperature is not so sensitive to the combinations of tap holes when two matte tap holes are employed. In addition, as larger fractions of the low temperature zones appear when the M3 tap hole is in use, it is then suggested to select the combinations of the other three holes while to avoid the M3 as much as possible for the matte tapping operation, in order to achieve a better result of both melt flow and temperature.

4 Conclusions

1) A CFD simulation was carried out with CFX 4.3 to study the melt flow and temperature distributions in the 1-to-1 (one slag exit adopted with one matte tap hole) and 1-to-2 (one slag exit adopted with two matte tap holes) modes of the matte tapping operation. Terms of the “dead zone” and “low temperature zone” are defined for qualitative and quantitative comparisons of the results in different operation modes.

2) The melt flows in the settler are similar in both the 1-to-1 and the 1-to-2 operation modes, that is, the chaotic flow exists mainly in the inlet centre and the flow in most part of the settler is uniform across the cross-section, with low velocity zone concentrated in the middle whilst high velocity regions mainly along the two side walls. As a result, the melt will take a shortcut to the slag exit, which is not desired in practice.

3) Evident circulations are found in the 1-to-2 operation mode, due to higher flow rate and stronger flow of the melt along the settler’s sides. Therefore, it is more likely to cause a shortcut of the melt to the slag exit of the settler.

4) Combinations of the slag and matte tap holes have significant effects on the temperature distributions of the melt. The matte temperature gradually decreases when the selected tap holes become further away to the inlet in the 1-to-1 operation mode, whilst the melt temperature is more uniform along the settler in the 1-to-2 mode.

5) To avoid the shortcuts as well as to reduce the dead zone of the melt flow, the southern slag exit (the one is farther away from the matte tap holes) and the farthest matte tap hole (the M4 tap hole) are suggested to adopt. However, the M3 tap hole is suggested to avoid as much as possible for the matte tapping operation, in order to achieve a better distribution of both melt flow and temperature.

Acknowledgement

Acknowledgement is given to Jinlong Copper Co., Ltd., TongLing, China, for their great technical supports of the research. Many thanks are also given to the High Performance Computing Centre of Central South University, China, for the great supports of computing resources.

References

[1] MOSKALYK R R, ALFANTAZI A M. Review of copper pyrometallurgical practice: Today and tomorrow [J]. Mineral Engineering, 2003, 16(10): 893−919.

[2] JORGENSEN F R A, KOH P T L. Combustion in flash smelting furnace [J]. Journal of Metallurgy, 2001, 53(5): 16−20.

[3] LI Xin-feng, PENG Shi-heng, HAN Xiang-li, MEI Chi, XIAO Tian-yuan. Influence of operation parameters on flash smelting furnace based on CFD [J]. Journal of University of Science and Technology Beijing, 2004, 11(2): 115−119. (in Chinese)

[4] SOLNORDAL C B, JORGENSEN F R A, KOH P T L, HUNT A. CFD modelling of the flow and reactions in the Olympic dam flash furnace smelter reaction shaft [J]. Applied Mathematical Modelling, 2006, 30(11): 1310−1325.

[5] GUI Wei-hua, WANG Ling-yun, YANG Chun-hua, XIE Yong-fang, PENG Xiao-bo. Intelligent prediction model of matte grade in copper flash smelting process [J]. Transactions of Nonferrous Metals Society of China, 2007, 17(5): 1075−1081.

[6] CHEN Hong-rong, MEI Chi. Operation optimization of concentrate burner in copper flash smelting furnace [J].Transaction of Nonferrous Metals Society of China, 2004, 14(3): 631−636. (in Chinese)

[7] XIE Kai. Several theory and operation optimization challenges in the development of modern copper flash smelters [D]. Changsha: Central South University, 2006. (in Chinese)

[8] KOH P T L, JORGENSEN F R A, ELLIOUT B J. Solids falling in flash furnace burner concentrate chutes [J]. International Journal Mineral Process, 2007, 83(3−4): 81−88.

[9] DEBRINCAT D P, SOLNORDAL C B, van DEVENTER J S J. Influence of particle properties on the size of agglomerated metallurgical powders [J]. International Journal of Mineral Process, 2008, 87: 17−27.

[10] DEBRINCAT D P, SOLNORDAL C B, van DEVENTER J S J. Characterisation of inter-particle forces within agglomerated metallurgical powders [J]. Powder Technology, 2008, 182(3): 388−397.

[11] HIGGINS D R, GRAY N B, DAVIDSON M R. Simulating particle agglomeration in the flash smelting reaction shaft [J]. Mineral Engineering, 2009, 22(14): 1251−1265.

[12] KEMORI N, SHIBATA Y, FUKUSHIMA K. Thermodynamic consideration for oxygen pressure in a flash smelting furnace at Toyo smelter [J]. Journal of Metallurgy, 1985, 37(5): 25−29.

[13] FAGERLUND K O, JALKANEN H. Microscale simulation of settler

processes in copper matte smelting [J]. Metallurgical Materials Transaction B, 2000, 31: 439−451.

[14] XIA J L, AHOKAINEN T, KANKAANPÄÄ T, JÄRVI J, TASKINEN P. Flow and heat transfer performance of slag and matte in the settler of a copper flash smelting furnace [J]. Steel Research International, 2007, 78: 155−159.

[15] ZHOU Ping, YU Jian-ping, CHEN Hong-rong, MEI Chi. Settling mechanism and influencing factors on matte droplets in settler slag of copper flash smelting furnace [J]. The Chinese Journal of Nonferrous Metals, 2006, 16(12): 2032−2037. (in Chinese)

[16] MEI Chi, ZHOU Jie-min, PENG Xiao-qi, ZHOU Nai-jun, ZHOU Ding. Simulation and optimization of furnaces and kilns for nonferrous metallurgical engineering [M]. Berlin Heidelberg: Springer; Beijing: Metallurgical Industry Press, 2010.

[17] YU Jian-ping. Analysis of matte settling mechanism and numerical simulation research on fluid field and temperature field in copper flash smelting settler [D]. Changsha: Central South University, 2006. (in Chinese)

闪速炉沉淀池中熔体流动特性的数值模拟

周 俊[1]，陈 卓[2,3]，周 萍[2,3]，余建平[2]，刘安明[4]

1. 中南大学 冶金科学与工程学院，长沙 410083；
2. 中南大学 能源科学与工程学院，长沙 410083；
3. 流程工业节能湖南省重点实验室，长沙 410083；
4. 金隆铜业有限公司，铜陵 244021

摘 要：采用 CFX4.3 对闪速炉沉淀池中的熔体流动和温度分布进行数值模拟研究。针对 1 个出渣口对应 1 个冰铜出口(1-to-1)与 1 个出渣口对应 2 个冰铜出口(1-to-2)这两种操作方案共设立 16 种计算工况。模拟结果表明，两种方案下熔体流动相似，但采用 1-to-2 操作方案时，熔池中可见明显的回流。仿真中还发现，渣口与冰铜出口的不同组合方式对沉淀池中熔体温度分布的影响显著，其中在 1-to-2 操作方案下，沉淀池中的熔体温度更均匀。在实际生产中，当采用远离沉淀池入口的放铜口进行操作时将更有利于实现沉淀池内熔体温度的均匀分布。

关键词：CFD 模拟；熔体流动；熔体温度；熔炼池；闪速熔炼

(Edited by YANG Hua)